A Liquid Sensor based on Frequency Selective Surfaces

Peter M. Njogu, Benito Sanz-Izquierdo and E.A. Parker

***Abstract*—A novel, simple and easy-to-fabricate liquid sensor using frequency selective surfaces (FSS) is proposed. The new sensor concept is based on modifying the capacitance between adjacent FSS elements when materials of different electrical characteristics are inserted. The change in capacitance produces a change in resonant frequency. The FSS design consists of a 9 x 9 array of square loops on 0.31λ x 0.31λ square unit cells with trenches between the loops. The trenches are filled with liquids under test (LTU). The structure operates at 4.6 GHz without any liquid. When liquids are inserted in the trenches, the resonance frequency varies in relation to the dielectric constant of the liquid. This is observed by measuring the transmission coefficient (S_{21}). Butan-1-ol, ethanol, methanol, propan-2-ol, and Xylene are used to demonstrate the sensing function. A maximum sensitivity of 8.65 % for Xylene was achieved. Further, very low differences were observed between the measured and expected dielectric constant and loss tangent, thus validating the design. The device is inexpensive, compact, and easy to make and scalable for large area operations in liquid detection for microwave sensing applications. This technique has potential applications in reconfigurable FSS.**

***Index Terms*—Dielectric, frequency selective surface (FSS), liquid, material characterization, permittivity, sensor**

I. INTRODUCTION

Any material is characterized by its electrical properties in terms of complex permittivity and permeability. These can determine its electromagnetic response and their potential employment in specific industrial applications. Liquids are a type of material with a wide range of applications, including in the biomedical sector [1] [2]. The methods for sensing and determining the electrical properties of liquids are continuously evolving [3] .

Microwave sensors have gained popularity due to their simplicity, inexpensive fabrication, and ease of use. One widespread technique is to use a resonating structure for determination of complex permittivity of the material. They operate on the principle of measuring the complex permittivity through analysis of the fundamental resonance frequency shift in the transmission/reflection response. At single or discrete set of frequencies, resonant technique offers potential for accurate measurements. Waveguide, dielectric, and coaxial cavity resonators have traditionally been employed for materials characterization [4] [5]. The material to be characterized is inserted in the cavity location where electric field is at its maximum causing cavity perturbation. The introduction of material results in changes in the resonant frequency of the cavity [3]. Exploiting this phenomenon, several sensing devices have been developed. In [6], a planar substrate integrated waveguide cavity resonator is presented where microfluidic capillaries are used for the insertion of the material. This method is also employed in [7] and [8] with the implementation of a split ring resonator with a microfluidic channel. The split ring and capillary concepts are combined in [9] where a complementary split ring resonator (CSRR) is presented for dielectric characterization of liquids. This is further developed in [10] where an open complementary split-ring resonator is employed with a slot container. In [11], dual mode, quarter ring microstrip resonators microfluidic sensor with capillary are used. In [12], a sensor that exploits excitation of a resonant mode within a cavity containing a minute sample of a liquid is presented. In [13], an RFID sensor is presented for identification and evaluation of liquid chemical based on the shift in the resonant frequency of an applied UHF RFID chipped tag.

Metamaterials are artificially constructed composites that exhibits electromagnetic properties that are difficult to achieve using conventional or naturally occurring materials [14] and includes electromagnetic band-gap (EBG) structures [15] and FSS [16]. They have recently been used for sensing liquids. In [17] [18] and [19], metamaterial absorber sensors are proposed where an air gap between a copper plate and backside resonator is used to fill chemicals liquids. EBGs have recently been employed in wireless sensor design in [20] by creating trenches between adjacent cells. This concept was advanced in [21] using a Casero Fractal design element.

In general, these liquid sensors provide good sensitivity and accuracy, but they also present design and operational complexities, and bulkiness while others are delicate and requires intricate assembly. Their design structure requires complicated measurement setups followed by complex design construction. Further costs accrue due to additional drilling and cutting for microfluidic subsystems. Extra parts e.g., capillaries, capsules and liquid containers would then be needed which further increases the costs. Others EBG based [20] [21] are two parts designs, which must be intricately assembled beside the design complexity. A single unit, easy to make and use sensor implies simplicity, lower cost, and ease of assembly.

This paragraph of the first footnote will contain the date on which you submitted your paper for review. It will also contain support information, including sponsor and financial support acknowledgment. For example, "This work was supported in part by the U.S. Department of Commerce under Grant BS123456".

The authors are with the University of Kent, School of Engineering and Digital Art, Canterbury CT2 7NZ, UK (e-mail: pmn20@kent.ac.uk; b.sanz@kent.ac.uk; e.a.parker@kent.ac.uk).

Frequency Selective Surfaces (FSS) are electromagnetic filtering structures usually consisting of arrays of periodic conductors [22] [23] on a suppoting dielectric material. They are a type of metamaterial [24]. Frequency selective surfaces modify the incoming electromagnetic signal in relation to their instrinsic resonant frequency. Their responses are dependent on the geometry and spacing of the element, dielectric material thickness and properties as well that of its surroundings [23]. This property can be used to develop conact-less sensors. FSS sensors have been designed to monitor structural health [25] [26] and [27], sensing of temperature and strain [28], breathing [29], strain [30] and dielectric characterization [31] [32].

In this paper, a Frequency Selective Surface (FSS) based sensor for sensing liquids falling onto a surface is proposed. In the new concept outlined in this work, the sensing function is achieved by altering the capacitance between adjacent FSS elements when materials of different electrical characteristics are inserted in trenches. The change in capacitance produces a change in the frequency resonance, which is detected as transmission response of the FSS. Trenches were dug in the dielectric around the conductors. The basic principle of operation of the proposed sensor is the excitation of a resonant mode of the FSS with the trenches filled with different liquids under test (LUT). The FSS sensor operates at about 4.6 GHz with a broad range of frequencies in relation to the LUT. To the best of authors' knowledge, this is the first design based on the FSS structure for sensing of liquids. The proposed sensor is scalable and can be re-designed to operate in different frequency bands. The motivation is the creation of a wireless sensor for the detection of liquids falling into a surface. The main application is on the detection on medium to large surfaces that can be adjusted by the array size. Curve fitting approach is employed to estimate the LUT complex permittivity and sensitivity analysis based on the shifted parameters. The rest of this paper is organized as follows. Section II details the geometry of the unit cell, the integrated trenches, and its characteristic behavior. Section III details fabrication and measurements of the design while section IV discusses the performance evaluation of the proposed sensor. Finally, section V discusses the conclusion.

II. FSS SENSOR/DETECTOR DESIGN

A. The FSS Sensor Unit Cell Design

The FSS was designed, simulated and tested using CST Microwave Studio™. For simplicity, the FSS was simulated as an infinite structure using a unit cell with periodic boundaries. Fig. 1(a) depicts the geometry of the unit cell of the FSS sensor design. A band stop FSS was selected as changes in the sensors could be observed through nulls in the transmission responses. In terms of element, a square loop FSS was used because it offers dual polarization and good angle of incidence behavior.

In the design, the square loops were made of copper and the substrate was RT/Duroid 5880 of thickness 3.175 mm, dielectric constant, ε_r of 2.2 and loss tangent (tan δ) of 0.0009. The cell had 1 mm wide and 2 mm deep trenches around its edges. The trenches were introduced through the partial removal of the substrate around the square loop as shown in Fig. 1(b). The trenches reduce the amount of dielectric material which decreases the permittivity and losses of the FSS in free space. The unit cell and the square loop dimensions were optimized to operate at 4.6 GHz. The gap x between the conductor loop and the edge of the unit cell is 1 mm. The periodicity, P, of the square loop array is the sum of g, the gap between adjacent loops and d_2 the length of the conductor. d_1 is the length of the unit cell element. The design dimensions are shown in Table 1. Fig. 2 shows the simulated transmission response of the FSS for angle of incidence at 0° incidence, 45° TE and 45° TM incidence, respectively. TE denotes the E-plane response whereas TM denotes H-plane response. Resonance of the unit cell occurred at normal incidence with a frequency of 4.6 GHz with no appreciable frequency drift at TE 45° and TM 45° i.e., 45° off broadside illumination for TE and TM polarization.

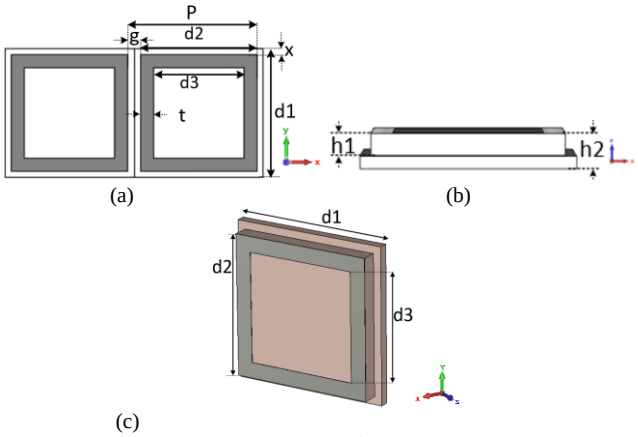

Fig. 1(a) the top view and dimensions of the FSS cell (b) the cross-sectional view (c) the perspective view

TABLE I
THE UNIT CELL DIMENSIONS

Parameter	d_1	d_2	d_3	P	g	x	t	h_1	h_2
Value (mm)	20	18	14	20	2	1	2	2	3.175

B. The Square Loop Operations and Equivalent circuit

The square loop FSS has band reject frequency response dependent on its physical dimensions [33]. It is a relatively simple shape and ideal to build a prototype for performance assessment or application. The equivalent circuit (EC) of the square loop FSS has been investigated by [34] [35] [36]. Fig. 3(a) presents the equivalent circuit (EC) of the square loop band stop filter. The EC model provides a simple and fast method of FSS analysis that is supported by transmission line analogy in which equivalent capacitive (C_i) and inductive (L_i) lumped components construct of the FSS can be calculated. η is the characteristic intrinsic impedance of free space equal to 377Ω. The proposed FSS array is symmetrical with periodicity P and a gap g between two adjacent conductor loops. It can be represented as lumped elements consisting of capacitance (C_i) and Inductance (L_i). Gap g represents the capacitive elements while the length of the conductor represents the inductive element. Resonance occurs when the perimeter of the loop is approximately one wavelength. The inductance and capacitance values determine the resonance frequency, ω and as in

$$\omega = \frac{1}{\sqrt{L_i C_i}} \quad (1)$$

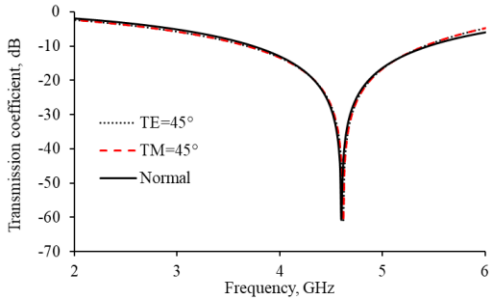

Fig. 2 Simulated transmission responses of the loop FSS

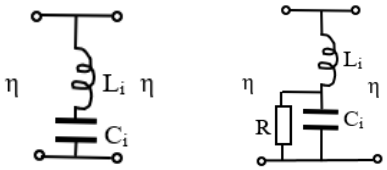

(a) (b)

Fig. 3 Equivalent circuit models: a) the square loop FSS (b) the FSS with a lossy liquid in the trenches

The dielectric material affects the reflection or transmission responses. With a finite thickness, the dielectric material effect on the FSS structures can be explained using the equivalent circuit analysis. The designed inductive FSS is a square loop of width t. Its intrinsic capacitance C_i and inductance, L_i, for TE incident wave can be approximated from path capacitance and strip inductance using (2) and (5) respectively, a conducting strips approximation developed by [37] that enables the calculation of L_i and C_i values. For transverse electrical (TE) incidence wave, the vertical strips of the FSS act as a L_i impedance in the EC, and the horizontal gratings as a C_i impedance [33] of

$$\mathrm{Ci} = \frac{2\mathrm{P}}{\eta\pi c}\left\{\mathrm{In}\left(\mathrm{cosec}\left(\frac{\pi \mathrm{g}}{2\mathrm{P}}\right) + \mathrm{G}(\lambda, \mathrm{g}, \mathrm{P})\right\}\right. \quad (2)$$

where Ci is the intrinsic capacitance between adjacent loops, determined by periodicity P and the gap g between adjacent loops. $G(\lambda, g, P)$ is a correction term expressed by

$$G = \left\{\frac{Q_2 cos^4(\frac{\pi g}{2P})}{1+Q_2 \sin^4\left(\frac{\pi g}{2P}\right)} + \frac{1}{16}\left(\frac{P}{\lambda}\right)^2\left(1 - 3\sin^2\left(\frac{\pi g}{2P}\right)\right)^2 \cos^4\left(\frac{\pi g}{2P}\right)\right\} \quad (3)$$

and the factor Q_2 is given by

$$\mathrm{Q_n} = \frac{1}{\sqrt{1-(\frac{2\mathrm{P}}{\mathrm{n}\lambda})^2}} - 1 \quad (4)$$

where the value of n in this case is 2.

To approximate the strip inductance, L_i, the g in the correction term, (3), is substituted by t, and Li results in

$$\mathrm{L_i} = \frac{\eta\lambda^2}{32\mathrm{P}\pi c\left\{\mathrm{In}\left(\mathrm{cosec}\left(\frac{\pi t}{2P}\right)+\mathrm{G}(\lambda,\mathrm{t},\mathrm{P})\right)\right\}} \quad (5)$$

where L_i is the strip inductance determined by conductors of periodicity P, width t, c is the speed of light and η is the impedance of free space.

From (2) and (5), the theoretical component values for free-standing FSS are L_i = 3.8114 nH and C_i = 214.26 fF. This capacitance needs to be adjusted due to the effect of dielectric.

In one-sided substrate, the capacitance increases proportional to the effective relative permittivity [23], [38] given by

$$\varepsilon_{eff} = \frac{\varepsilon_r+1}{2} \quad (6)$$

Although (6) is a general equation for the cases when the substrate is sufficiently thick (> λ/5) [33], it can be a good approximation in the case of square loops even in substrates of thicknesses of about 0.05λ [39]. Therefore, using (6), the resulting capacitance when compensated by the dielectric substrate is C_i = 342.9 fF. The resonant frequency for this LC circuit is approximately 4.5 GHz, which is within the expected 5% error margin of the frequency of 4.3 GHz for the FSS obtained from the simulation of the dielectric loaded FSS (no trenches).

In liquid sensing, the dielectric losses of the liquids in the trenches can be high. These losses can be represented as a resistor in parallel with the capacitor as shown in Fig. 3(b).

C. Parametric Analysis

Parametric study was conducted to determine the behaviour of the FSS for varying empty trenches' depth (h_1), from 0.0 mm to 3.0 mm, at 0.5 mm intervals. Fig. 4 shows the effect of changing trench depth (h_1) on resonant frequency and the corresponding capacitance. In our model, the inductance is constant (L_i = 3.8114 nH) [22]. The capacitance has been calculated using the frequency obtained in simulations and equation (1). As expected, removing dielectric material decreases the effective permittivity and capacitance, and increases the resonant frequency. The capacitance as a function of depth, h_1, follows the fitted equation

$$C_i = -3.7778h_1^3 + 25.143h_1^2 - 58.103h_1 + 359.76 \text{ fF} \quad (7)$$

To assess the potential behavior of the proposed FSS structure (Fig. 1) as a liquid sensor, a simulation was carried with the trenches filled with materials of various dielectric constants, and loss tangents. Fig. 5 illustrates the FSS structure indicating the sections of the design with liquid. In the initial study, shown in Fig.6 and Fig. 7, the dielectric permittivity was varied from 1 to 20, and the loss tangent was fixed at 0. The resonant frequency decreased with increase of the dielectric constant. From (1), capacitance, C_i due to liquids of varying ε_r values in the trenches was obtained and is also shown in Fig. 7. C_i increases linearly with ε_r as

$$C_i = 33.312\varepsilon_r + 288.89 \text{ fF} \quad (8)$$

The effect of changes in loss tangent on the transmission response and resonance frequency are shown in Fig. 8 and Fig. 9 respectively. The permittivity of the liquid was kept at 8 while the loss tangent was varied between 0 and 0.9.

The depth of the null in the transmission coefficient curve decreases with the increase in loss tangent. A small decrease in resonant frequency is also observed, with a maximum of about 6% shift for a value of tan δ of 0.9.

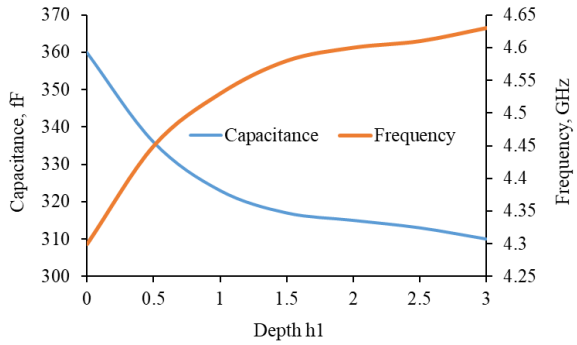

Fig. 4 A plot of capacitance and frequency vs the trench depth

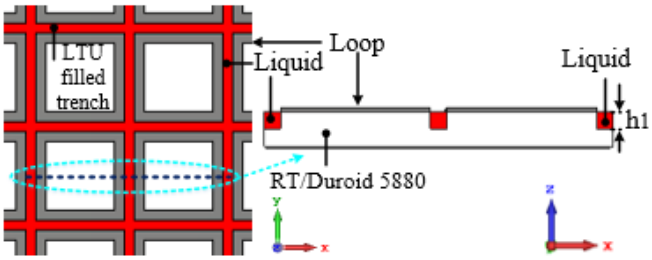

(a) (b)

Fig. 5 The (a) top view and (b) cross sectional view of a section of the FSS sensor liquid-filled trenches

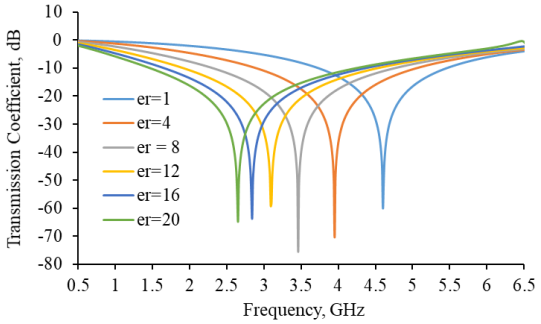

Fig. 6 S_{21} of the FSS with liquid of various e_r in the trenches

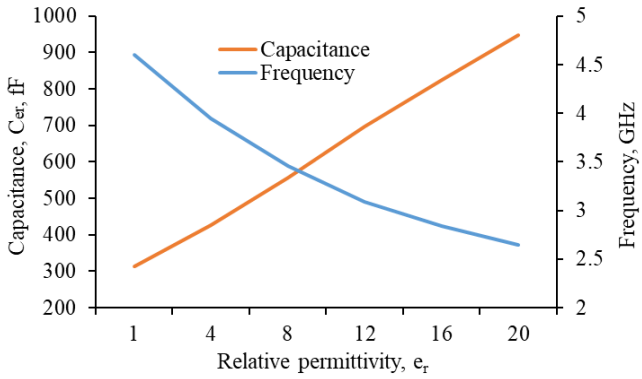

Fig. 7 Permittivity e_r vs frequency and capacitance

D. *Sensor study for readily available liquids*

Five chemical liquids were used to authenticate the sensing/detecting functionality of the proposed design. These were Butan-1-o1, Propan-2-o1, Ethanol, and Methanol whose dielectric properties at 5 GHz and 20°C were obtained from [40] and Xylene from [41] and are shown in Table II. Fig 10 shows the S_{21} of the unit cell elements when the trenches are filled with the different LUT.

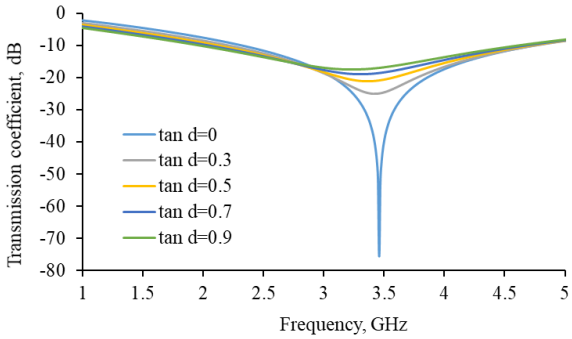

Fig. 8 Simulated dependence of transmission coefficient (S21) of the FSS loss tangent (tan δ) of the liquid in the trenches (ε_r = 8)

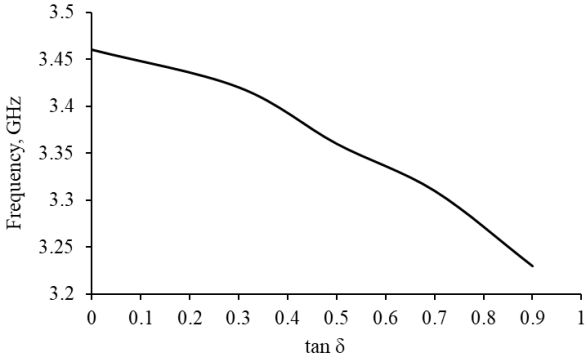

Fig. 9 Sensitivity of the FSS structure: simulated dependence of the resonant frequency on loss tangent (tan δ).

III. *Fabrication and Measurements*

A. *Fabrication*

The FSS unit cell with dimensions as in Fig.1 and Table I was extended to a 9 x 9 array to create a prototype of the sensor. The model of the sensor is shown in Fig. 11 with the liquid-filled trenches depicted in red colour. It has a 5mm wide edge to hold the liquids inside and for mechanical purposes, making a total dimension of 192 mm x 192 mm. The prototype was fabricated at Printech Circuit Laboratories [42] using standard printed circuit boards (PCBs) procedures. It was then milled using a high precision milling machine to create the trenches around the loops. The fabricated sensor is shown in Fig. 12 (a) while Fig. 12 (b) shows the milled trenches.

B. *Measurements and Results*

Using a Marconi Instruments microwave test set 6204B and in a plain wave chamber, the insertion loss of the FSS was measured with empty trenches. Fig 12 (c) shows the measurements set up. The trenches were then filled using a syringe with the correct amount of liquid (14 ml) and the transmission response (S_{21}) measured. The FSS structure was kept horizontal using a bubble level to ensure that the liquid was uniform throughout the structure. The S_{21} results are shown in Fig. 13. Table III tabulates both the simulated and measured resonance frequency (f_s) and the frequency shift (Δf) from the reference of the LUT. The resonance frequency for both the simulated and measured show frequency shift towards lower frequencies from the reference frequency i.e., air resonance. This agrees with similar observation in [43] and [44]. The resonance points shifts to the lower frequencies when the

TABLE II
ELECTRICAL CHARACTERISTICS OF THE LUT's

Liquid	Relative permittivity ε_r	Loss tangent (tan δ)
Butan-1-o1	3.29	0.47
Propan-2-o1	3.8	0.64
Ethanol	5.08	0.96
Methanol	12.42	0.65
Xylene	2.57	0.018

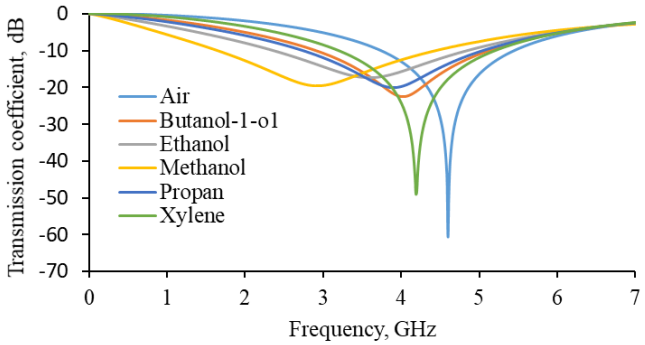

Fig. 10 The simulated frequency response of the proposed sensor structure for the various LUT

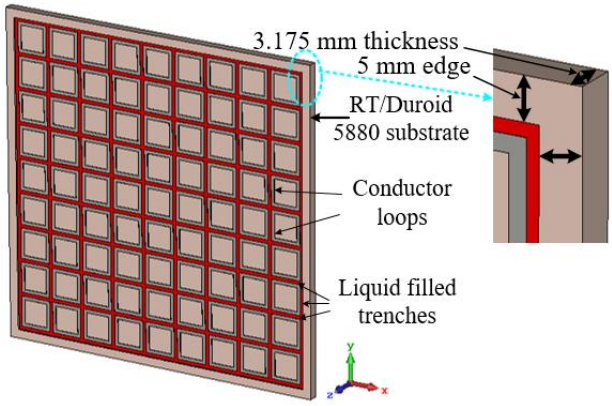

Fig. 11 The perspective view of the FSS sensor prototype with liquid filled trenches

trench is filled with liquids of high dielectric constant. The differences between simulated and measured results could be due to fabrication errors, potential loss of liquid when inserting into the trenches, quality of the LUT, and possible differences in the permittivity values of LUT from those given in [40].

IV. PROPOSED SENSOR PERFORMANCE EVALUATION

A. *Sensitivity Analysis*

The proposed design performance evaluation was conducted with the integrated fluidic trenches on the FSS filled with the five different liquids of different electrical properties described in section II. The sensitivity (S) as a performance parameter was used to evaluate the sensor performance according to the criterion proposed in [21] and [44]. To estimate the sensitivity (S) of the device, air filled trenches were chosen as the reference. The proposed criterion gives the mathematical expression of the sensitivity, S, of

$$S = \frac{\Delta f / f_s}{\Delta \varepsilon} \quad (9)$$

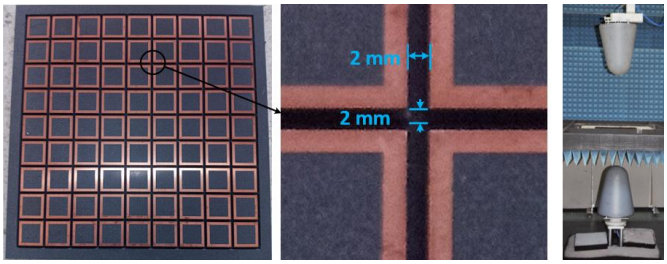

(a) (b) (c)

Fig. 12: (a) The fabricated the FSS sensor (b) the empty trenches (c) the measurement set-up

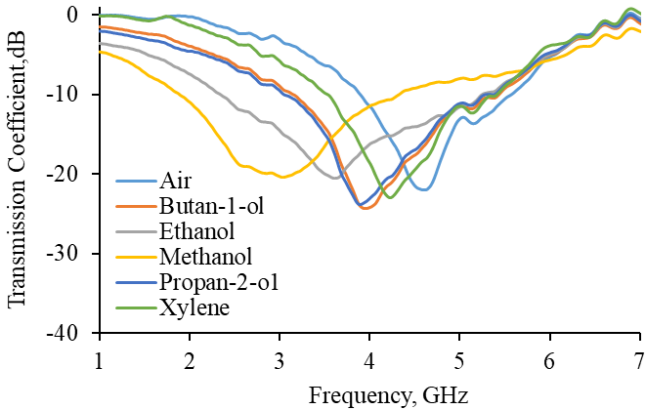

Fig. 13 The measured frequency response of the proposed sensor structure for the various LUT

TABLE III
MEASURED RESONANCE FREQUENCY AND FREQUENCY SHIFT

LUT	f_s GHz		Δf GHz	
	Simulated	Measured	Simulated	Measured
Butan-1-o1	4.02	3.92	0.58	0.68
Ethanol	3.59	3.61	1.01	0.99
Methanol	2.92	3.01	1.68	1.59
Propan-2-o1	3.9	3.83	0.7	0.77
Xylene	4.19	4.24	0.41	0.36

Δf is expressed as $(f_o - f_s)$ where f_o and f_s are the resonance frequency of the FSS when filled with air and the LUT respectively. $\Delta\varepsilon$ is $(\varepsilon_s - \varepsilon_o)$ where ε_s and ε_o are dielectric constant of the LUT in the trench and air respectively. Table IV shows the frequency shift and the computed sensitivity (S) of the various LUTs.

B. *Material dielectric characterization*

The complex permittivity (ε_r) and loss tangent $(tan\ \delta)$ of the LUT were calculated using mathematical models derived using polynomial curve fitting technique [2] and [21]. The necessary equations that best fit the given data set were generated to a 3rd degree for greater accuracy. The resonating frequency (f_s) and bandwidth of frequency shifting (Δf) were used to determine the dielectric constant and loss tangent of the LUT respectively to a good degree of accuracy. The relationship between the resonating frequency variations with respect to the change in the dielectric values of LUT was expressed using the third-order polynomial expression

$$\varepsilon_r = -1.6763 f_s^3 + 24.8613 f_s^2 - 121.5387 f_s + 198.7187 \quad (10)$$

TABLE IV
THE MEASURED PERFORMANCE ANALYS IS OF SENSOR

LUT	Resonance Frequency (GHz)	Frequency Shift (GHz)	Sensitivity (%)
Air	4.6	-	-
Butanol-1-o1	3.92	0.68	7.58
Ethanol	3.61	0.99	6.72
Methanol	3.01	1.59	4.63
Propan-2-o1	3.83	0.77	7.18
Xylene	4.24	0.36	8.65

where ε_r is the calculated real permittivity and f_s is the LUT resonating frequency. The relationship between the bandwidth of frequency shifting and loss tangent (tan δ) was mathematically derived as a 3rd order polynomial as the best-fit of the given dataset and is expressed by

$$tan\,\delta = -2.0252\Delta f^3 + 4.3111\Delta f^2 - 1.3509\Delta f + 0.0395 \quad (11)$$

where tan δ is the calculated loss tangent and Δf is the LUT frequency shift from the reference.

From the equations (8) and (9), the dielectric constant and loss tangent of samples of LUT of unknown permittivity and loss tangent were calculated and compared to the actual published values to validate the data. The calculated values of ε_r and $tan\,\delta$ are shown in Table V. The calculated results demonstrate a good agreement with actual permittivity and loss tangents values of all the LUT. The root mean square error between the actual and the calculated permittivity and loss tangent was also calculated. The highest error of 1.7% and 3.3% for dielectric tangent and loss tangent respectively validate the performance of the device. The error could be due to scattering parameters of the microwave sensor being influenced by electric and magnetic properties of its surroundings, which can be reflected in the insertion loss S_{21} of the resonator. Impurities and analytes in the trench can have effect on the amplitude as well as the resonance frequency of the sensor *[2]*. It is noticeable from the results that resonance point of Butanol-1-o1 and Propan-2-o1 are almost indistinguishable. This is because of their close dielectric parameters. This implies that the effectiveness of the sensor is dependent on the differences between the dielectric parameters of the LUTs.

TABLE V
CALCULATED DIELECTRIC PROPERTIES THE LUT

LUT	Dielectric constant (εr)			Loss tangent (tan δ)		
	Actual	Calculated	RMS Error (%)	Actual	Calculated	RMS Error (%)
Air	1	-	-	-	-	-
Butanol-1-o1	3.29	3.3416	1.6	0.47	0.4776	1.6
Ethanol	5.08	5.0959	0.31	0.96	0.9624	0.25
Methanol	12.42	12.4189	0.009	0.65	0.6498	0.03
Propan-2-o1	3.8	3.7357	1.7	0.64	0.6308	1.4
Xylene	2.57	2.5651	0.19	0.018	0.0174	3.3

*Root mean square (RMS) computed as $\frac{\sqrt{(Actual-Calculated)^2}}{Actual}$

V. DISCUSSION AND CONCLUSION

A new concept for microwave liquid sensor based on Frequency Selective Surfaces has been demonstrated. The sensor uses trenches between FSS elements to modify the transmission response when liquids with different permittivity are inserted. A mathematical model was developed for determination of the dielectric constant and loss tangent of the LUT. The evaluated complex permittivity and loss tangent are in good agreement with the actual values. The highest errors in the measured values of the dielectric constant and dielectric loss are within 1.7% for Propan-2-o1 and 3.3% for Xylene respectively. This demonstrates that the proposed microwave sensor is suitable as a low-cost platform for the detection of liquids with good sensitivity and low detection error. Table VI summarizes the performance analysis of the reported metamaterial EBG detectors closest to the proposed design. It shows that, besides its simplicity, it offers higher sensitivity and thus improved detection performance.

The developed sensor is ideal for instances requiring robust, real-time monitoring at low-cost and complexity, low-power consumption and with simple fabrication techniques. The independent resonant nature due to each chemical allows the device to be reused for different and various liquids. The contactless nature of the detection process makes it suitable for a safe working environment. For example, it can be used in industrial processes where dangerous chemicals may need to be identified. Furthermore, the size of the FSS sensor can be scaled up or down as required. Previous work [45] has indicated that even a unit cell is able to produce a transmission response by adjusting the distance of the antennas used for testing.

Fig. 14 illustrates a potential set up integrated in a wireless sensor network. The sensor is set in such a way that liquids can fall into the FSS structure. To ensure the uniformity of the liquid during the measurements, a bubble level should be used during the installation to prevent erroneous readings. The sensor has a flat surface which means that some droplets may remain on the surface outside the trenches which may affect measurements. A future version of the design is envisaged where cells could be three dimensional with a slight slope to allow droplets to be guided towards the trenches.

Note that this is the first concept and the reading setup is the standard for FSS measurements. However, a more compact arrangement could be developed in the future where the antennas and system only target the specified frequency band of operation. In addition, in an industrial environment, a dedicated space would be desirable.

Even though the main application described here is on liquid sensing, the structure and design have potential applications in reconfigurable FSS using low-loss liquids such as the one employed in [46].

ACKNOWLEDGMENT

The authors would like to thank Mr. A. Mendoza for setting up the chamber for measurement and Andrew Brookman for facilitating the fabrication of the milled sensor at Printech Circuit Laboratories Ltd. This work was funded by the EPSRC grant titled Low-Profile Ultra-Wideband WideScanning Multi-Function Beam-Steerable Array Antennas (EP/S005625/1) and and the Royal Society - International Exchanges 2019 Cost Share (NSFC) (Ref: IEC\NSFC\191780)

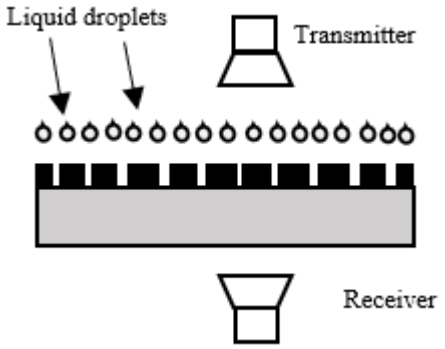

Fig. 14 Illustrative potential FSS sensor application

TABLE VI
COMPARISON OF THE PROPOSED DESIGN WITH THE REPORTED METAMATERIAL BASED SENSING DESIGNS

Parameter	[21](EBG)	[20] (EBG)	This work (FSS)
Resonant Frequency (GHz)	2.45	2.45	4.6
Construction	Complex	Complex	Simple
Maximum Measured Sensitivity	0.875	-	8.65
Minimum frequency shift Δf (GHz)	0.054	-	0.68

REFERENCES

[1] A. Ebrahimi, J. Scott and K. Ghorbani, "Microwave reflective biosensor for glucose level detection in aqueous solutions," *Sensors and Actuators A: Physical*, vol. 301, 2020.

[2] A. A. M. Bahar, Z. Zakaria, M. K. M. Arshad, A. A. M. Isa, Y. Dasril and R. A. Alahnomi, "Real Time Microwave Biochemical Sensor Based on Circular SIW Approach for Aqueous Dielectric Detection," *scientific reports* , vol. 9, pp. 1-12, 2019.

[3] L. F. Chen, C. K. Ong, C. P. Neo, V. V. Varadan and V. K. Varadan, Microwave Electronics Measurements and Materials Characterization, Chichester: John Wiley & Sons Ltd, 2004.

[4] B. A. Galwas, J. K. Piotrowski and J. Skulski, "Dielectric Measurements Using a Coaxial Resonator Opened to a Waveguide Below Cut-Off," *IEEE TRANSACTIONS ON INSTRUMENTATION AND MEASUREMENT*, vol. 46, no. 2, pp. 511-514, 1997.

[5] H. Lobato-Morales, A. Corona-Chávez, D. V. B. Murthy and J. L. Olvera-Cervantes, "Complex permittvity measurements using cavity perturbation technique with substrate integrated waveguide cavities," *REVIEW OF SCIENTIFIC INSTRUMENTS*, vol. 81, pp. 1-4, 2010.

[6] K. Saeed, R. D. Pollard and I. C. Hunter, "Substrate Integrated Waveguide Cavity Resonators for Complex Permittivity Characterization of Materials," *IEEE Transactions on Microwave Theory and Techniques*, vol. 56, no. 10, pp. 2340 - 2347, 2008.

[7] A. A. Abduljabar, D. J. Rowe, A. Porch and D. A. Barrow, "Novel Microwave Microfluidic Sensor Using a Microstrip Split-Ring Resonator," *IEEE TRANSACTIONS ON MICROWAVE THEORY AND TECHNIQUES*, Vols. 62,, no. 3, pp. 679-688, 2014.

[8] D. J. Rowe, S. al-Malki, A. A. Abduljabar, A. Porch, D. A. Barrow and C. J. Allender, "Improved Split-Ring Resonator for Microfluidic Sensing," *IEEE Transactions on Microwave Theory and Techniques*, vol. 62, no. 3, pp. 689 - 699, 2014.

[9] E. L. Chuma, Y. Iano, G. Fontgalland and L. L. B. Roger, "Microwave Sensor for Liquid Dielectric Characterization Based on Metamaterial Complementary Split Ring Resonator," *IEEE Sensors Journal* , vol. 18, no. 24, pp. 9978 - 9983, 2018.

[10] C.-S. Lee, B. Bai, Q.-R. Song, Z.-Q. Wang and G.-F. Li, "Open Complementary Split-Ring Resonator Sensor for Dropping-Based Liquid Dielectric Characterization," *IEEE Sensors Journal*, vol. 19, no. 24, pp. 11880 - 11890, 2019.

[11] A. A. Abduljabar, N. Clark, J. Lees and A. Porch, "Dual Mode Microwave Microfluidic Sensor for Temperature Variant Liquid Characterization," *IEEE Transactions on Microwave Theory and Techniques*, vol. 65, no. 7, pp. 2572 - 2582, 2017.

[12] A. J. Cole and P. R. Young, "Chipless Liquid Sensing Using a Slotted Cylindrical Resonator," *IEEE Sensors Journal*, vol. 18, no. 1, pp. 149 - 156, 2018.

[13] V. Makarovaite, A. J. R. Hillier, S. J. Holder and J. C. Batchelor, "Passive Wireless UHF RFID Antenna Label for Sensing Dielectric Properties of Aqueous and Organic Liquids," *EEE SENSORS JOURNAL*, vol. 19, no. 11, pp. 4299-4307, 2019.

[14] S. S. Bukhari, J. Vardaxoglou and W. Whittow, "A Metasurfaces Review: Definitions and Applications," *Applied Science- MDPI*, vol. 9, pp. 1-14, 2019.

[15] N.Christopoulos, G.Goussetis, A.P.Feresidis and J.C.Vardaxoglou, "Metamaterials With Multiband AMC And EBG Properties," in *2005 European Microwave Conference*, Paris, France, 2005.

[16] F. Bayatpur and K. Sarabandi, "Tuning Performance of Metamaterial-Based Frequency Selective Surfaces," *IEEE Transactions on Antennas and Propagation* , vol. 57, no. 2, pp. 590 - 592, 2009.

[17] Y. I. Abdulkarim, L. Deng, O. Altıntaş, E. Ünal and M. Karaaslan, "Metamaterial absorber sensor design by incorporating swastika shaped resonator to determination of the liquid chemicals depending on electrical characteristics," *Physica E: Low-dimensional Systems and Nanostructures*, vol. 114, pp. 1-9, 2019.

[18] Y. I. Abdulkarim, L. Deng, H. Luo, S. Huang, M. Karaaslan, O. Altıntas, M. Bakır, F. F. Muhammadsharif, H. N. Awl, C. Sabah and K. S. L. Al-badri, "Design and study of a metamaterial based sensorfor the application of liquid chemicals detection," *Journal of Materials Research and Technology*, vol. 9, no. 5, pp. 10291-10304, 2020.

[19] Y. I. Abdulkarim, L. Deng, M. Karaaslan, O. Altıntas, H. N. Awl, F. F. Muhammadsharif, C. Liao, E. Unal and H. Luo, "Novel Metamaterials-Based Hypersensitized Liquid Sensor Integrating Omega-Shaped Resonator with Microstrip Transmission Line," *Sensors MDPI*, vol. 20, no. 3, pp. 1-18, 2020.

[20] S. Y. Jun, B. S. Izquierdo and E. A. Parker, "Liquid Sensor/Detector Using an EBG Structure," *IEEE Transactions on Antennas and Propagation* , vol. 67, no. 5, pp. 3366 - 3373, 2019.

[21] A. Arif, A. Zubair, K. Riaz, M. Q. Mehmood and M. Zubair, "A Novel Cesaro Fractal EBG-Based Sensing Platform for Dielectric Characterization of Liquids," *IEEE TRANSACTIONS ON ANTENNAS AND PROPAGATION*, vol. 69, no. 5, pp. 2887-2895, 2021.

[22] E. A. Parker, "THE GENTLEMAN'S GUIDE TO FREQUENCY SELECTIVE SURFACES," 17 04 1991. [Online]. Available: https://kar.kent.ac.uk/59863/. [Accessed 27 04 2021].

[23] B. A. MUNK, FREQUENCY SELECTIVE SURFACES Theory and Design, New York: JOHN WILEY & SONS, INC. , 2000.

[24] J. Yiannis and C. Vardaxoglou, "Metamaterial arrays and applications: FSS, EBG & AMC structures," in *2014 International Workshop on Antenna Technology: Small Antennas, Novel EM Structures and Materials, and Applications (iWAT)*, Sydney, NSW, Australia, 2014.

[25] F. H. W. Mustaffa, S. N. Azemi, M. F. Jamlos, A. A. Al-Hadi and P. J. Soh, "Frequency Selective Surface for Structural Health Monitoring," *IOP Conference Series: Materials Science and Engineering*, vol. 318, pp. 1-9, 2018.

[26] D. Pieper, K. M. Donnell, O. Abdelkarim and M. A. ElGawady, "Embedded FSS sensing for structural health monitoring of bridge columns," in *2016 IEEE International Instrumentation and Measurement Technology Conference Proceedings*, Taipei, Taiwan, 2016.

[27] S.-D. Jang, B.-W. Kang and J. Kim, "Frequency selective surface based passive wireless sensor for structural health monitoring," *Smart Materials and Structures*, vol. 22, pp. 1-7, 2013.

[28] M. Mahmoodi and K. M. Donnell, "Novel FSS-based sensor for concurrent temperature and strain sensing," in *2017 IEEE International*

Symposium on Antennas and Propagation & USNC/URSI National Radio Science Meeting, San Diego, CA, USA, 2017.

[29] S. Milici, J. Lorenzo, A. Lázaro, R. Villarino and D. Girbau, "Wireless Breathing Sensor Based on Wearable Modulated Frequency Selective Surface," *IEEE SENSORS JOURNAL*, vol. 17, no. 5, pp. 1285-1292, 2017.

[30] S. Soltani, P. S. Taylor, E. A. Parker and J. C. Batchelor, "Popup Tunable Frequency Selective Surfaces for Strain Sensing," *IEEE Sensors Letters*, vol. 4, no. 4, pp. 2475-1472, 2020.

[31] F. Costa, C. Amabile, A. Monorchio and E. Prati, "Waveguide Dielectric Permittivity Measurement Technique Based on Resonant FSS Filters," *IEEE MICROWAVE AND WIRELESS COMPONENTS LETTERS*, vol. 21, no. 5, pp. 273-275, 2011.

[32] M. Mahmoodi and K. M. Donnell, "Performance Metrics for Frequency Selective Surface-Based Sensors," *IEEE Sensor Letters*, vol. 1, no. 6, pp. 1-4, 2017.

[33] D. Ferreira, R. F. S. Caldeirinha, I. Cuiñas and T. R. Fernandes, "Square Loop and Slot Frequency Selective Surfaces Study for Equivalent Circuit Model Optimization," *IEEE TRANSACTIONS ON ANTENNAS AND PROPAGATION*, vol. 63, no. 9, pp. 3947-3955, 2015.

[34] R. J. Langley and E. A. Parker, "Equivalent circuit model for arrays of square loops," *ELECTRONICS LETTERS*, vol. 18, no. 7, pp. 294-296, 1982.

[35] C. K. Lee and R. J. Langley, "Equivalent-circuit models for frequency-selective surfaces at oblique angles of incidence," *IEE PROCEEDINGS*, vol. 132, no. 6, p. 395 – 399, 1985.

[36] A. E. YILMAZ and M. KUZUOGLU, "Design of the Square Loop Frequency Selective Surfaces with Particle Swarm Optimization via the Equivalent Circuit Model," *RADIO ENGINEERING*, vol. 18, no. 2, pp. 95-102, 2009.

[37] N. Marcuvitz, Waveguide Handbook, London: Peter Peregrinus, 1986.

[38] F. Costa, A. Monorchio and G. Manara, "Efficient Analysis of Frequency-Selective Surfaces by a Simple Equivalent-Circuit Model," *IEEE Antennas and Propagation Magazine*, vol. 54, no. 4, pp. 35 - 48, 2012.

[39] P. Callaghan and E. A. Parker, "Element dependency in dielectric tuning of frequency selective surfaces," *Electronics Letters*, vol. 28, no. 1, p. 42 – 44, 1992.

[40] A. P. Gregory and R. N. Clarke, "Tables of the Complex Permittivity of Dielectric Reference Liquids at Frequencies up to 5 GHz," National Physical Laboratory, 2012.

[41] CEM, "Solvent Choice for Microwave Synthesis," 01 06 2021. [Online]. Available: https://cem.com/uk/microwave-chemistry/solvent-choice. [Accessed 01 06 2021].

[42] Printech Circuit Laboratories, "Printech Circuit Laboratories," Printech Circuit Laboratories, 20 08 2021. [Online]. Available: https://www.pcbs.space/. [Accessed 20 08 2021].

[43] A. C. d. C. Lima, E. A. Parker and R. J. Langley, "Tunable frequency selective surface using liquid substrates," *Electronics Letters*, vol. 30, no. 4, pp. 281 - 282, 1994.

[44] H. Lobato-Morales, D. V. B. Murthy, A. Corona-Chavez, J. L. Olvera-Cervantes, J. Martinez-Brito and L. G. Guerrero-Ojeda, "Permittivity Measurements at Microwave Frequencies Using Epsilon-Near-Zero (ENZ) Tunnel Structure," *IEEE TRANSACTIONS ON MICROWAVE THEORY AND TECHNIQUES*, vol. 59, no. 7, pp. 1863 - 1868, 2011.

[45] E. A. Parker, J. -B. Robertson, B. Sanz-Izquierdo and J. C. Batchelor, "Minimal size FSS for long wavelength," *ELECTRONICS LETTERS*, vol. 44, no. 6, p. 394 – 395, 2008.

[46] C. Song, E. L. Bennett, J. Xiao, R. P. Tianyuan Jia, K.-M. Luk and Y. Huang, "Passive Beam-Steering Gravitational Liquid Antennas," *IEEE TRANSACTIONS ON ANTENNAS AND PROPAGATION* , vol. 68 , no. 4, pp. 3207-3212, 2020.

Peter Njogu is Ph.D. research student in electronic engineering with the University of Kent, Canterbury, U.K. His research interests include wearable antennas, multiband antennas, millimetre wave antennas and 3-D printed antennas.

Benito Sanz Izquierdo received the B.Sc. from ULPGC (Spain), and the M.Sc. and Ph.D. degrees from the University of Kent, U.K. He was Research Associate with the School of Engineering, University of Kent, in 2013, became lecturer in Electronic Systems and, in 2018, Senior Lecturer. In 2012, he worked for Harada Industries Ltd where he developed novel antennas for the automotive industry. His research interests are multiband antennas, wearable electronics, additive manufacturing (3D printing), substrate integrated waveguides components, metamaterials, sensors, electromagnetic band-gap structures, frequency selective surfaces and reconfigurable devices.

Edward (TED) A. Parker received the M.A. degree in physics and the Ph.D. degree in radio astronomy from the St. Catharine's College, University of Cambridge, Cambridge, U.K. He was appointed as a Reader with the University of Kent, Canterbury, U.K., in 1977, where he has been a Professor of Radio Communications, since 1987. He is currently a Professor Emeritus with the University of Kent. He established the Electronics Laboratory, Antennas Group, University of Kent. He is a member of the Livery of the Worshipful Company of Scientific Instrument Makers, London, U.K. His current research interests include the application of frequency selective surfaces and the study and overhaul of antique clocks. He is a member of the Institution of Engineering and Technology.